Sodium-ion pickup observed above the magnetopause during MESSENGER's first Mercury flyby: Constraints on neutral exospheric models

Menelaos Sarantos,[1] James A. Slavin,[1] Mehdi Benna,[2] Scott A. Boardsen,[1,3] Rosemary M. Killen,[4] David Schriver,[5] and Pavel Trávníček[5]

Received 2 October 2008; revised 23 December 2008; accepted 21 January 2009; published 25 February 2009.

[1] Single-particle tracings of sodium pickup ions launched upstream of Mercury's magnetopause are used to investigate the access of these ions to the magnetosphere and set limits on the distribution of neutral sodium about the planet during the first MESSENGER flyby. The transport of pickup ions is modeled using flow velocity and magnetic fields from a three-dimensional magnetohydrodynamic simulation. Extensive penetration of pickup ions into the magnetosphere is found in the post-noon and dusk local time sectors due to the northward interplanetary magnetic field at the time of MESSENGER's first flyby. It is concluded that: (1) pickup of magnetosheath photoions may be an important source of hot planetary ions within the magnetosphere; and (2) the sodium ions in the magnetosheath observed by MESSENGER must originate from an extended neutral exosphere due to ion sputtering and/or to a partially escaping distribution generated by photon-stimulated desorption with yields modified by regolith trapping. **Citation:** Sarantos, M., J. A. Slavin, M. Benna, S. A. Boardsen, R. M. Killen, D. Schriver, and P. Trávníček (2009), Sodium-ion pickup observed above the magnetopause during MESSENGER's first Mercury flyby: Constraints on neutral exospheric models, *Geophys. Res. Lett.*, *36*, L04106, doi:10.1029/2008GL036207.

1. Introduction

[2] Observations by the Fast Imaging Plasma Spectrometer (FIPS) on the MErcury Surface, Space ENvironment, GEochemistry, and Ranging (MESSENGER) spacecraft, obtained during the probe's first Mercury flyby on January 14, 2008, show that Mercury's magnetosphere is surrounded by ions originating from the planetary exosphere and extending above the magnetopause [*Zurbuchen et al.*, 2008]. Although the plasma observations probably include substantial contributions from magnesium ions, the most abundant ion species was sodium, whose spatial distribution peaked at closest approach and exhibited secondary maxima in the magnetosheath [*Zurbuchen et al.*, 2008; *Slavin et al.*, 2008]. The exospheric neutral sodium atoms about Mercury, known since the mid-1980s, have been hypothesized to constitute an important source of ions for the magnetosphere [e.g., *Delcourt et al.*, 2003].

[3] The sodium exosphere is refilled by atoms ejected via photon-stimulated desorption (PSD), meteoroid impact vaporization, thermal desorption, and sputtering by the solar wind [e.g., *Killen et al.*, 2007]. Spatial variations result from the superposition of separate source processes: viz., impact vaporization is likely isotropic, ion sputtering is associated with polar cusp areas at latitudes poleward of about ±40°, and PSD has a strong dependence on solar zenith angle. Exospheric gradients critically affect the distribution of magnetospheric Na^+ ions [*Delcourt et al.*, 2003].

[4] Photoions originating at altitudes above the magnetopause rapidly pick up thermal speeds comparable to the bulk flow speed of Mercury's magnetosheath whence they originate. *Slavin et al.* [2008] suggested that the penetration of magnetosheath pickup ions into the magnetosphere might be the cause of a boundary layer feature observed just prior to MESSENGER's outbound magnetopause crossing. In the following we examine the spatial origin and transport of sodium pickup ions in the context of the MESSENGER measurements in order to: (a) ascertain their role in magnetospheric processes, including stress balance at the magnetopause and possible boundary layer formation; and (b) constrain the global topology of the neutral sodium exosphere.

2. Models of Mercury's Magnetosphere and Exosphere During the MESSENGER Flyby

[5] The interplanetary magnetic field (IMF) B was directed outward from the Sun with a northward component during the January 14, 2008, MESSENGER flyby [*Slavin et al.*, 2008]. For our purposes the magnetosphere of Mercury is described by a multi-fluid magnetohydrodynamic (MHD) model [*Benna et al.*, 2008]. The input conditions for this run were: n_{sw} = 20 cm^{-3}, V_{sw} = 400 km/s including an aberration angle of ~6° due to planetary motion, and IMF [B_x, B_y, B_z] = [−12, 12, 5] nT, where n_{sw} and V_{sw} are the solar wind density and velocity, respectively. A non-centered dipole moment of ~229 nT was assumed [*Anderson et al.*, 2008]. Given the Magnetometer measurements and the choice of model dipole, the solar wind parameters were selected so that the simulated magnetopause and bow shock boundaries agree with MESSENGER observations.

[6] The magnetosphere contributes to the production of energetic neutrals and ions via sputtering caused by bombardment of the surface by solar wind ions as shown in

[1]Heliophysics Science Division, NASA Goddard Space Flight Center, Greenbelt, Maryland, USA.
[2]Solar System Exploration Division, NASA Goddard Space Flight Center, Greenbelt, Maryland, USA.
[3]Goddard Earth Sciences and Technology Center, University of Maryland, Baltimore County, Baltimore, Maryland, USA.
[4]Department of Astronomy, University of Maryland, College Park, Maryland, USA.
[5]Institute of Geophysics and Planetary Physics, University of California, Los Angeles, California, USA.

0094-8276/09/2008GL036207$05.00

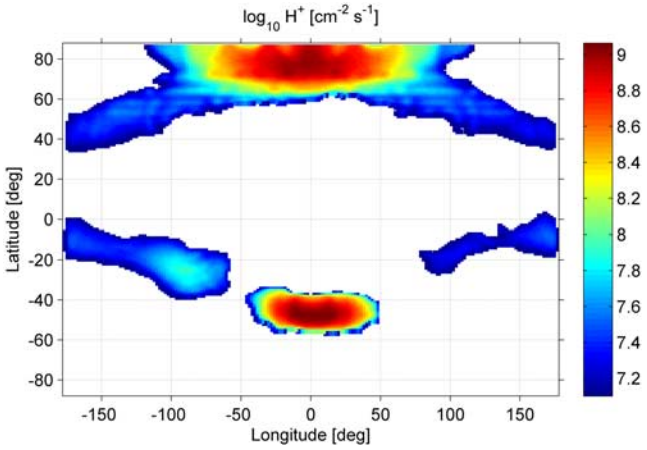

Figure 1. The flux of solar wind protons bombarding the surface of Mercury is obtained from the MHD model of *Benna et al.* [2008]. The north-south asymmetry of ion precipitation is suggestive of the enhanced sodium tail that was observed over the northern hemisphere at the time of the first MESSENGER flyby [*McClintock et al.*, 2008].

Figure 1. The modeled incident flux exhibits a north-south asymmetry with the northern cusp being more directly "connected" to the solar wind as expected in the case of an anti-sunward IMF B_x component [e.g., *Sarantos et al.*, 2001; *Kallio and Janhunen*, 2003]. A total of 1.3×10^{25} and 2.5×10^{25} ions s^{-1} precipitate onto the dayside southern and northern cusps, respectively. The 2:1 ratio is consistent with kinetic modeling results for a strong radial IMF [*Kallio and Janhunen*, 2003]. Extensive precipitation on auroral latitudes is seen, as also shown by *Kallio and Janhunen* [2003].

[7] A parameterized model of Mercury's exosphere, including the source processes of ion sputtering, PSD, and thermal desorption, was presented by *Mura et al.* [2007]. Each source was treated independently due to the collisionless nature of the exosphere. A critical model parameter is the velocity distribution with which sodium atoms are released from the surface. For ion sputtering the ejecta are assumed to follow a Sigmund-Thompson distribution function [see *Mura et al.*, 2007, equation (6)]. The PSD distribution has interchangeably been described as a Weibull function having a tail of non-thermal atoms [see *Mura et al.*, 2007, equation (11)], or, ignoring the high-energy tail, as a Maxwellian function having the mean temperature of 1,500 K. The resulting altitude profiles differ markedly, as sodium atoms from the first two distributions reach distances far from the planet. The fraction of sputtered atoms escaping Mercury varies from 50–80% (ion sputtering), to 10–20% (Weibull PSD), down to ~1% (Maxwellian PSD), with variations attributed to the changing radiation acceleration pressure along Mercury's orbit.

[8] We obtain the distribution of atomic sodium about Mercury during the MESSENGER encounter from the parametric fits listed in Table 1 of *Mura et al.* [2007]. For sputtering the impact proton rate was scaled from the 5×10^{24} s^{-1} tabulated there to our own 1.3×10^{25} s^{-1}, while a sputtering yield of 0.1, a binding energy of $E_b = 2$ eV, and a sodium surface content of $f_{Na} = 0.0053$ were assumed. For the Maxwellian PSD a temperature of 1,500 K was assumed, while for the Weibull PSD a radiation acceleration of $\alpha = 1.92$ m s^{-2} and a heliocentric distance of r = 0.35 astronomical units (AU) were employed.

[9] Possible neutral sodium distributions from these processes are shown in Figure 2 projected onto the X-Z and X-Y Mercury Solar Orbital (MSO) planes. Superimposed are magnetic field-line tracings from the MHD model indicating the approximate boundaries of the magnetopause and the bow shock. Sputtering (Figure 2a) and PSD that includes a tail distribution of very energetic atoms (Figure 2b) place neutrals at altitudes above the magnetopause, while a Maxwellian PSD (Figure 2c) is expected to contribute little to the ion pickup measurements. The model-predicted subsolar zenith column abundance out to 3 R_M in each case is (a) 3.9×10^9, (b) 3.9×10^{11}, and (c) 7.2×10^{11} Na atoms cm^{-2}, respectively. Subsolar zenith column abundances of a few times 10^{10}–10^{11} atoms cm^{-2} are reported from ground-based telescopic observations (see review by *Killen et al.* [2007]).

[10] Neither thermal desorption nor impact vaporization contributions are considered here. The former process, similar to the Maxwellian PSD, yields thermal atoms

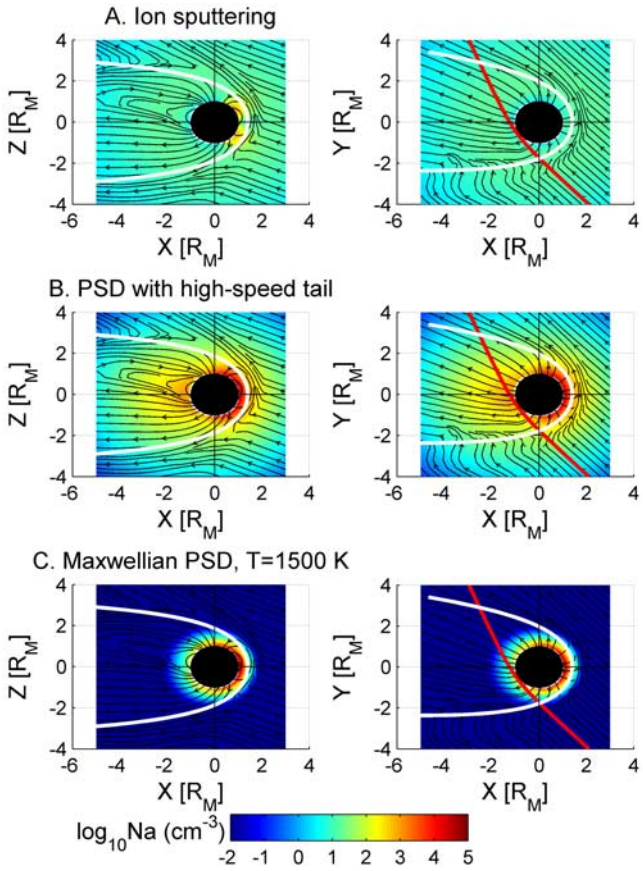

Figure 2. Sodium exospheric density including the source processes of (a) ion sputtering, (b) PSD described by a Weibull distribution function, and (c) PSD described by a Maxwellian distribution function. Magnetic field-line tracings, obtained from the MHD model, indicate the magnetospheric boundaries. The red line follows MESSENGER's trajectory. The white line indicates the magnetopause fit by *Slavin et al.* [2009].

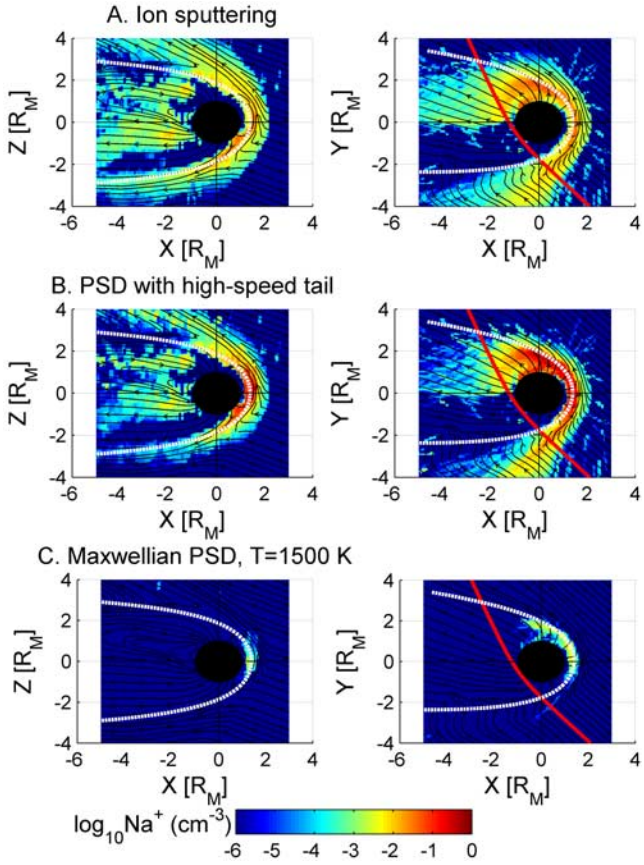

Figure 3. The distribution of sodium pickup ions resulting from each neutral source process. The ions are initialized according to the source distributions of Figure 2, and their subsequent transport in the MHD fields is followed using single-particle tracing. Magnetospheric ions and ions launched beyond X = 2 R_M are not considered.

resulting in ions that mainly recycle to the surface. The latter process, usually described as a Maxwellian source with T ~ 3000 K, was not parameterized and is expected to produce 10–20% of the total exospheric Na.

3. Distribution of Sodium Pickup Ions

[11] The model exosphere provides the weight factors for the Na^+ test particles, which are subsequently followed in the fields of the MHD simulation. Approximately 10^5 test particles were launched from locations sampled every 0.1 R_M (where R_M is Mercury's radius) in the area delineated by the approximate locations of the magnetopause and the bow shock. The simulation box extends to ±4 R_M in the Y and Z directions and to 5 R_M in the anti-sunward tail to include the greater part of MESSENGER's traversal of the magnetosphere. The test particles, which are initially assumed to have zero velocity, are followed for ~2 min by which time most have escaped the simulation box or impacted the surface. Particles that penetrate well into the magnetosphere and which subsequently have relatively large residence times of ~8 min [*Delcourt et al.*, 2003] are discontinued. The photoionization rate for sodium of 4.83×10^{-5} s^{-1} used here is the theoretical value for quiet solar conditions, 5.92×10^{-6} s^{-1} at Earth [*Huebner et al.*, 1992], scaled to Mercury's solar distance at the flyby of 0.35 AU.

[12] The spatial distribution of pickup Na^+ density resulting from each source is depicted in Figure 3. For this IMF configuration the electric field in the magnetosheath is dawnward. Consequently, heavy ions with large gyroradii are pushed deep into the magnetosphere on the dusk side, but less so at dawn as seen by the clear dawn-dusk asymmetry in the simulation. Ion densities of $\leq 10^{-3}$ cm^{-3}, $\sim 10^{-2}$ cm^{-3}, and 0.1–1 cm^{-3} are predicted for Maxwellian PSD, sputter, and Weibull PSD sources, respectively, right behind the nose of the bow shock. These are approximately an order of magnitude higher than the densities expected due to the local ionization source because ions originating close to the Sun-Mercury line, where the magnetosheath flow comes to a stagnation point, are accelerated only gradually.

[13] The mean energy of the modeled pickup ions is shown in Figure 4. Particles having energies of 10–100 keV are expected along the trajectory of MESSENGER. These are sufficiently energetic to enter the field of view of the plasma spectrometer, especially on the inbound (dusk) side, where the instrument's pointing is favorable. Ions close to the Sun-Mercury line are less energetic, consistent with the magnetosheath convection flow slowing there.

4. Discussion

[14] A source of energization up to 10 keV of planetary sodium ions has previously been described by *Delcourt et*

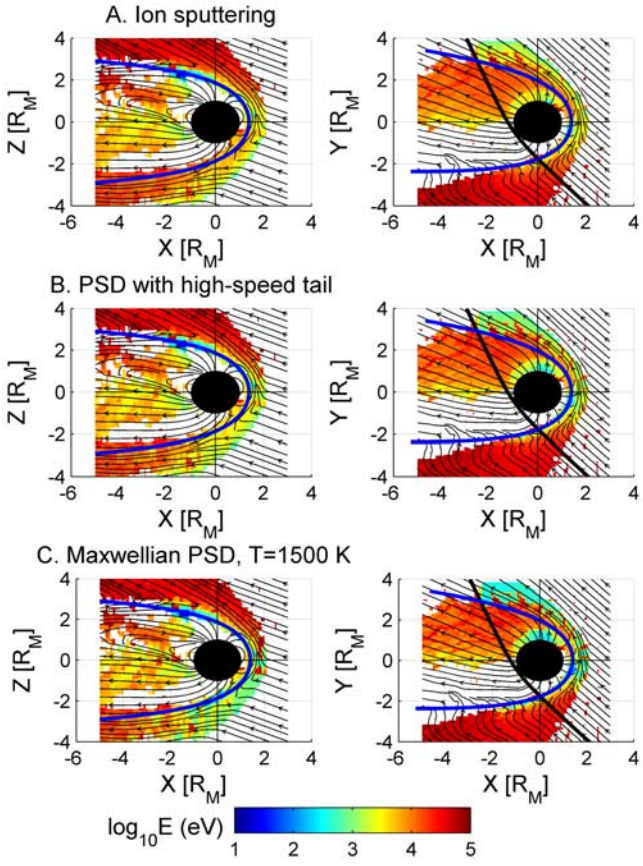

Figure 4. North-south and equatorial slices of the mean energy per bin of sodium pickup ions.

al. [2003]. They showed that Speiser-type trajectories resulting from $E \times B$ drifting of heavy ions from polar regions to areas close to the equatorial plasma sheet are expected at Mercury due to the large magnetic field gradients close to the planet. Evidently the pickup process results in comparable if not higher energies. However, the energization of plasma-sheet-trapped ions is slow, i.e., on timescales of ~8 min. Therefore these trajectories are unstable to rapid reconfigurations of the magnetosphere expected on timescales of ~1–2 min, the typical timescales for solar wind variability at Mercury. In contrast, the energization of pickup ions by the fast magnetosheath flow is quick (<1 min) and leads to penetration of energetic ions into the dusk (dawn) magnetosphere for northward (southward) IMF.

[15] The distribution of sodium pickup ions is clearly affected by exospheric gradients. The Maxwellian PSD neutral component is gravitationally bound and contributes less than 10^{-6} pickup ions cm^{-3} during the inbound and outbound "legs" of the MESSENGER flyby. In that sense the observation by MESSENGER of a secondary peak of relative Na^+ counts in the magnetosheath at $X \sim -5$ R_M suggests the presence of an escaping neutral component either due to ion sputtering or due to a Weibull PSD.

[16] The modeled sodium ion density near the magnetospheric boundaries provides clues to the possible extent of mass loading at Mercury. The solar wind–comet interaction paradigm suggests that substantial slowing of the solar wind would result from the addition of just 1% of heavy ion mass to the solar wind (e.g., review by *Coates* [1995]). This amount of sodium ions alone ($\geq$0.1 ions cm^{-3}) can be provided by the Weibull PSD source distribution in the region in front of the magnetopause and behind the bow shock (Figure 3b). Substantial modifications to Mercury's magnetospheric topology would be expected if the sodium exosphere were to be described by this term. However, the observations by Mariner 10 and MESSENGER seem consistent with terrestrial-like bow shock and magnetopause standoff distances and shapes given the expected solar wind pressure and intrinsic field magnitude [*Slavin et al.*, 2009]. Additionally, no ion cyclotron waves in resonance with heavy planetary ions were observed by Mariner 10 [*Boardsen and Slavin*, 2007] and none were reported from the first MESSENGER flyby. These findings all imply a magnetosphere that is at best weakly loaded with thermalized heavy ions of planetary origin.

[17] On the basis of this argument, we conclude that the Weibull PSD source distribution yields an unrealistic escaping coma. However energetic the parent neutral ejection process is, interaction with individual grains of the porous surface (regolith trapping) tends to "thermalize" the ejecta [*Cassidy and Johnson*, 2005]. The resulting scale height of the sodium exosphere (~150 km) should be sufficiently low that sodium ions alone will not lead to efficient mass loading through the pickup process described here.

[18] A related interpretation would be that the PSD yield used in the *Mura et al.* [2007] model is too high. The laboratory-measured PSD yields [*Yakshinskiy and Madey*, 1999] would overestimate Mercury's sodium abundance as shown by *Killen et al.* [2001], partly because the yield from a porous regolith is one-third of the laboratory rate [*Cassidy and Johnson*, 2005]. PSD yields more than an order of magnitude lower than the experimental yields were found to be consistent with the lunar sodium exosphere abundances when the Moon's surface is shielded from precipitating ions by the terrestrial magnetosphere, while the PSD yield increased to approximately one-sixth of the laboratory yield when the Moon is exposed to the solar wind beyond the Earth's magnetopause [*Sarantos et al.*, 2008]. The effect is likely caused by ion-enhanced grain diffusion and/or by chemical sputtering [*Mura et al.*, 2009], and would apply to Mercury only along the cusp areas. The five to ten-fold reduction of the PSD yield used in the Weibull PSD model would result in ion densities below those expected to mass load the upstream solar wind.

5. Conclusions

[19] For the northward IMF conditions that held during the first MESSENGER flyby the tracings show strong pickup and entry into the magnetosphere with a maximum in the post-noon and dusk local time sectors where the magnetosheath electric field points toward the magnetopause. Pickup by the fast magnetosheath flow creates sodium ions with energies of ~10–100 keV whose dynamic pressure may displace the dawn-side magnetopause as suggested by *Slavin et al.* [2009]. If the much weaker pickup ion entry along the dawn flank of the magnetopause is sufficient to produce the boundary feature identified by *Anderson et al.* [2008] and *Slavin et al.* [2008], then much stronger effects would be expected along the dusk flank. This region will not be observed until after MESSENGER enters its orbital phase in 2011.

[20] During MESSENGER's first Mercury flyby the dayside neutral sodium measurements were contaminated by light reflected from the surface [*McClintock et al.*, 2008], so the distribution of sodium pickup ions is an indirect means of constraining the morphology of the neutral sodium cloud. The sodium ion measurements by MESSENGER at high altitudes prior to entering the magnetosphere [*Zurbuchen et al.*, 2008] are energetic pickup ions and strongly suggest significant contributions to the neutral exosphere at altitudes beyond the magnetopause by ion sputtering and by PSD.

[21] The PSD exosphere has been simulated using both a Maxwellian and a Weibull velocity distribution function. It is found that the former has negligible contributions to the pickup ion population, while the sodium pickup ions resulting from the latter distribution, which includes a tail of non-thermal neutrals, would substantially mass load the upstream solar wind contrary to what is observed by MESSENGER. The apparent absence of significant mass loading indicates that either the neutral sodium scale height is much lower than that predicted by a Weibull PSD term and/or that the actual PSD yields are much lower than those determined experimentally from flat surfaces. The ion distribution resulting from sputtered neutrals is similar to that from the Weibull PSD, although sodium ions from this distribution remain "trace" particles despite our assuming the moderately high yield of 0.1 per impact ion.

[22] **Acknowledgments.** The MESSENGER project is supported by the NASA Discovery Program under contracts NAS5-97271 to the Johns Hopkins University Applied Physics Laboratory and NASW-00002 to the Carnegie Institution of Washington.

References

Anderson, B. J., M. H. Acuña, H. Korth, M. E. Purucker, C. L. Johnson, J. A. Slavin, S. C. Solomon, and R. L. McNutt Jr. (2008), The structure of Mercury's magnetic field from MESSENGER's first flyby, *Science*, *321*, 82–85.

Benna, M., J. A. Slavin, M. Sarantos, D. N. Baker, M. E. Purucker, and S. Boardsen (2008), Comparative MHD models of the first two MESSENGER flybys of Mercury, *Eos Trans. AGU*, *89*(53), Fall Meeting Suppl., Abstract U21A-0039.

Boardsen, S. A., and J. A. Slavin (2007), Search for pick-up ion generated Na^+ cyclotron waves at Mercury, *Geophys. Res. Lett.*, *34*, L22106, doi:10.1029/2007GL031504.

Cassidy, T. A., and R. E. Johnson (2005), Monte Carlo model of sputtering and other ejection processes within a regolith, *Icarus*, *176*, 499–507.

Coates, A. J. (1995), Heavy ion effects on cometary shocks, *Adv. Space Res.*, *15*, 403–413.

Delcourt, D. C., S. Grimald, F. Leblanc, J.-J. Berthelier, A. Millilo, A. Mura, S. Orsini, and T. E. Moore (2003), A quantitative model of planetary Na^+ contribution to Mercury's magnetosphere, *Ann. Geophys.*, *21*, 1723–1736.

Huebner, W. F., J. J. Keady, and S. P. Lyon (1992), Solar photo rates for planetary atmospheres and atmospheric pollutants, *Astrophys. Space Sci.*, *195*, 1–289.

Kallio, E., and P. Janhunen (2003), Solar wind and magnetospheric ion impact on Mercury's surface, *Geophys. Res. Lett.*, *30*(17), 1877, doi:10.1029/2003GL017842.

Killen, R. M., A. E. Potter, P. Reiff, M. Sarantos, B. V. Jackson, P. Hick, and B. Giles (2001), Evidence for space weather at Mercury, *J. Geophys. Res.*, *106*, 20,509–20,525.

Killen, R. M., et al. (2007), Processes that promote and deplete the exosphere of Mercury, *Space Sci. Rev.*, *132*, 433–509.

McClintock, W. E., E. T. Bradley, R. J. Vervack Jr., R. M. Killen, A. L. Sprague, N. R. Izenberg, and S. C. Solomon (2008), Mercury's exosphere: Observations during MESSENGER's first Mercury flyby, *Science*, *321*, 92–94.

Mura, A., A. Milillo, S. Orsini, and S. Massetti (2007), Numerical and analytical model of Mercury's exosphere: Dependence on surface and external conditions, *Planet. Space Sci.*, *55*, 1569–1583.

Mura, A., P. Wurz, H. I. M. Lichtenegger, H. Schleicher, H. Lammer, D. Delcourt, A. Millilo, S. Orsini, S. Massetti, and M. L. Khodachenko (2009), The sodium exosphere of Mercury: Comparison between observations during Mercury's transit and model results, *Icarus*, in press.

Sarantos, M., P. H. Reiff, T. W. Hill, R. M. Killen, and A. L. Urquhart (2001), A B_x-interconnected magnetosphere model for Mercury, *Planet. Space Sci.*, *49*, 1629–1635.

Sarantos, M., R. M. Killen, A. S. Sharma, and J. A. Slavin (2008), Influence of plasma ions on source rates for the lunar exosphere during passage through the Earth's magnetosphere, *Geophys. Res. Lett.*, *35*, L04105, doi:10.1029/2007GL032310.

Slavin, J. A., et al. (2008), Mercury's magnetosphere after MESSENGER's first flyby, *Science*, *321*, 85–89.

Slavin, J. A., et al. (2009), MESSENGER observations of Mercury's magnetosphere during northward IMF, *Geophys. Res. Lett.*, *36*, L02101, doi:10.1029/2008GL036158.

Yakshinskiy, B. V., and T. E. Madey (1999), Photon-stimulated desorption as a substantial source of sodium in the lunar atmosphere, *Nature*, *400*, 642–644.

Zurbuchen, T. H., J. M. Raines, G. Gloeckler, S. M. Krimigis, J. A. Slavin, P. L. Koehn, R. M. Killen, A. L. Sprague, R. L. McNutt Jr., and S. C. Solomon (2008), Observations of Mercury's ionized exosphere and plasma environment, *Science*, *321*, 90–92.

M. Benna, Solar System Exploration Division, NASA Goddard Space Flight Center, 8800 Greenbelt Road, Greenbelt, MD 20771, USA.

S. A. Boardsen, M. Sarantos, and J. A. Slavin, Heliophysics Science Division, NASA Goddard Space Flight Center, 8800 Greenbelt Road, Greenbelt, MD 20771, USA. (menelaos.sarantos-1@nasa.gov)

R. M. Killen, Department of Astronomy, University of Maryland, College Park, MD 20742, USA.

D. Schriver and P. M. Trávníček, Institute of Geophysics and Planetary Physics, University of California, Los Angeles, CA 90024, USA.